PRELIMINARY RESULTS OF A JANUARY SIMULATION WITH AN IMPROVED VERSION OF THE GLAS MODEL

(J. Shukla, Y. Sud, and E. Sabatino)

Several aspects of the weaknesses and strengths of winter and summer simulations with the GLAS model are described in a recent paper by Halem et al. (1979), which points out that one of the weaknesses of the model is its lower evaporation over the oceans. This, along with smoothing of orography over high mountain peaks, was suspected to be responsible for weaker amplitudes of stationary waves in these simulations. We have introduced several modifications in the earlier version of the GLAS model. These were comprised of modified boundary layer calculations which led to an improvement in the fields of boundary layer fluxes and a stable calculation of surface temperature. This parameterization is discussed in a paper by Sud and Abeles (1979). In addition, the ground albedo over snow-ice covered surfaces of the earth are prescribed from an analysis of satellite observation of Matson (1978) and Rayner and Howarth (1977). This snow-ice data is combined with the bare land albedos of Posey and Clapp (1964). Furthermore, the model has been initialized for a long climate run by making the permanent ice depth equal to 3 meters and transient snow depth of 0-2 cm, depending upon its reflectivity. Sea surface temperatures from a 2° x 2° GFDL data set were interpolated to the 4° x 5° grid of the GLAS model. All the prescribed boundary conditions are now interpolated on a daily basis.

Furthermore, as a result of detailed examination of the code and the diagnostics of various calculations, a few additional modifications have been made. These consist of the following: elimination of Shapiro-filter on humidity field, maintaining conservations in strapping and unstrapping of cloud layer in the model, calling short wave radiation every half hour while maintaining long wave calls at 5-h frequency but with net radiative temperature modification to be made every half hour using the saved fluxes of long wave radiation, changes for correction of radiative heating rates over the mountains, and correcting a coding error in the interpolation of level-8 winds in the split-grid regions.

Preliminary results of first 31 days which consist of simulated month of January (starting from the initial conditions of 1 January 1975 from NMC analysis) are compared with the simulation with the earlier model run of Halem et al. (1979) of which February simulation has been presented in their paper. Some basic fields which show an impact from these changes are presented and compared with the earlier run.

Analysis of Results

An important result from these modifications was the improvement of one of the most serious deficiencies in the model, i.e., the lower amplitude of the stationary component of its general circulation. It is well known that the stationary waves are forced by diabatic heating sources and orography.

Since the earlier model produced an evaporation field which was significantly less than the observed over the oceans (Charney et al., 1977), an improvement in diabatic heating through increased boundary layer fluxes of evaporation and sensible heating over the oceans was expected to improve the stationary component of general circulation. This has happened in the new model simulation.

The following results compare the modified model with its earlier version. Figure captions (a) and (b) are used for the modified and earlier model results, respectively. Figs. 1a and 1b show the sea level pressure maps. Fig. 1a has better subtropical highs and a pronounced Siberian high. Also, the low over the coast of Japan is much better defined and the sea level pressure fields off the coast of Greenland have a better structure.

Figs. 2a and 2b show zonal plots of evaporation over the land and oceans in the two simulations. Increased evaporation over the oceans and lower evaporation over land in the modified model run are seen. This corrects a well known weakness of the model. Figs. 3 and 4 show the zonally averaged evaporation and precipitation fields. There is an increase in evaporation and precipitation in the new model.

An analysis of amplitude of stationary component of circulation geopotential height fields are presented. Tables 1a and 1b show the variance of geopotential height fields at the mandatory pressure levels. The values of variances for the new run compare well with the observations (as shown in Table 1c) of Oort and Rasmusson (1971) and show a considerable improvement over those of the old model shown in Table 1b. In Fig. 5 the plots of variance of geopotential height fields at 500 mb are shown. The new model results are in good agreement with observations. The peaks of variances in the baroclinic regions improve by a factor of two over the old model.

References

Charney, J. G., W. J. Quirk, S. H. Chow, and J. Kornfield, 1977: A comparative study of the effects of albedo changes on drought in semi-arid regions. J. Atmos. Sci., 34, 1366-1385.

Halem, M., J. Shukla, Y. Mintz, M. L. Wu, R. Godbole, G. Herman, Y. Sud, 1979: Comparisons of observed seasonal climate features with a winter and summer numerical simulation produced with the GLAS general circulation model. Report of the JOC Study Conf. on Climate Models: Performance, Intercomparison and Sensitivity Studies, GARP Publ. Series No. 22, 207-253, WMO, Geneva, Switzerland.

Matson, M., 1978: Winter Snow-Cover Maps of North America and Eurasia, 1966-1976.

Oort, A. H., and E. R. Rasmusson, 1971: Atmospheric circulation statistics. NOAA Prof. Paper 5, U.S. Dept. of Comm.

Posey, J. W., and P. F. Clapp, 1964: Global distribution of normal surface albedo. Geofisica Int'l., Vol. 4, 33-48.

References (Continued)

Rayner, J. N., and D. A. Howarth, 1977: Analysis of Spatial and Temporal Variation of the Ice in Antarctica. Vol. I-2, Final Report, Dept. of Geography and Inst. of Polar Studies, the Ohio State Univ., Columbus, Ohio.

Sud, Y., and J. Abeles, 1980: Calculation of surface temperature and surface fluxes in the GCM. Submitted to ASME for publication in Appl. Meteor. (Also in NASA Tech. Memo. (herein), Atmos. and Oceano. Res. Rev.-1979, NASA Goddard Space Flight Center, Greenbelt, Maryland.)

Table 1a.

MODIFIED MODEL

VARIANCE OF STATIONARY GEOPOTENTIAL HEIGHT(Z) FOR THE MONTH

SOUTHERN HEMISPHERE 10(GPM**2)

J A N U A R Y

P(MB)	90S	86S	82S	78S	74S	70S	66S	62S	58S	54S	50S	46S	42S	38S	34S	30S	26S	22S	18S	14S	10S	6S	2S
50.	0	66	384	662	1838	2418	2828	2631	2440	1553	907	450	231	182	171	152	118	90	75	91	80	70	70
100.	0	487	1082	1384	2289	2029	2147	2228	1566	1397	907	507	365	319	207	146	203	270	292	344	279	186	159
200.	0	81	226	226	238	411	524	923	1071	877	699	483	397	322	167	140	284	376	314	208	130	88	62
300.	0	9	94	35	73	91	163	435	628	586	550	428	377	310	168	91	127	177	144	86	48	27	18
400.	0	28	100	53	109	80	101	250	395	386	378	305	288	250	154	69	43	50	39	22	11	6	4
500.	0	22	58	32	65	59	68	151	249	249	238	200	202	186	129	64	33	26	17	12	8	4	2
700.	0	9	14	11	35	25	33	58	86	95	94	97	117	124	98	61	38	36	33	31	19	10	7
850.	0	4	21	37	38	26	33	34	40	43	53	77	103	108	96	76	58	53	46	37	25	17	14
900.	0	7	33	70	58	29	36	29	32	34	46	77	104	107	102	90	76	67	54	41	27	20	17
950.	0	11	53	122	91	35	36	30	31	31	45	82	110	113	118	120	116	102	74	56	37	27	22
1000.	0	17	81	188	138	49	37	31	32	32	48	90	120	124	140	162	172	152	105	78	50	35	29
MEAN	0	68	195	274	434	475	543	620	635	485	360	254	218	195	142	107	116	127	111	91	64	44	37

VARIANCE OF STATIONARY GEOPOTENTIAL HEIGHT(Z) FOR THE MONTH

NORTHERN HEMISPHERE 10(GPM**2)

J A N U A R Y

P(MB)	2N	6N	10N	14N	18N	22N	26N	30N	34N	38N	42N	46N	50N	54N	58N	62N	66N	70N	74N	78N	82N	86N	90N
50.	69	68	60	70	158	373	640	869	1109	1460	2016	2716	3491	4185	3987	3221	1941	1172	768	529	248	67	0
100.	146	175	235	350	634	1039	1495	1748	1514	1327	1919	2662	3220	3341	1065	2268	1520	772	554	465	208	95	0
200.	60	79	127	231	405	622	744	593	380	860	1859	2573	2678	2225	1590	1078	861	578	592	470	305	116	0
300.	18	25	45	86	169	219	243	188	449	1231	2104	2506	2298	1663	1145	869	907	593	515	390	281	90	0
400.	4	6	13	24	42	65	90	174	557	1192	1769	1917	1689	1179	850	693	788	483	382	254	194	59	0
500.	3	5	9	12	18	32	68	181	476	915	1267	1313	1156	805	608	507	581	339	266	162	126	40	0
700.	8	11	18	23	29	35	56	126	272	471	601	624	547	376	295	245	256	149	102	43	51	17	0
850.	14	15	19	20	21	26	40	79	180	304	413	428	366	269	224	142	136	103	66	32	33	9	0
900.	18	18	20	20	20	27	45	81	177	296	386	392	336	277	246	150	164	144	85	37	36	8	0
950.	21	23	27	27	23	31	58	93	193	291	377	383	321	302	313	213	240	223	155	52	40	6	0
1000.	27	30	40	42	32	41	78	113	221	315	392	391	339	358	423	326	365	346	278	85	55	6	0
MEAN	34	41	56	82	142	228	323	384	504	767	1191	1447	1495	1360	1157	883	704	446	342	227	145	49	0

Table 1b

EARLIER MODEL

VARIANCE OF STATIONARY GEOPOTENTIAL HEIGHT(Z) FOR THE MONTH

SOUTHERN HEMISPHERE 10(GPM**2)

J A N U A R Y

P(MB)	90S	86S	82S	78S	74S	70S	66S	62S	58S	54S	50S	46S	42S	38S	34S	30S	26S	22S	18S	14S	10S	6S	2S
50.	0	42	372	868	1305	1372	826	774	714	578	481	404	319	255	173	100	68	58	65	83	71	62	59
100.	0	566	837	1442	1242	597	960	948	669	489	402	444	510	379	253	170	142	143	132	155	125	82	80
200.	0	288	604	652	865	470	593	460	260	208	261	443	532	322	141	168	227	247	169	93	46	21	14
300.	0	91	237	312	327	297	390	301	176	213	318	499	572	347	122	80	101	117	78	42	19	9	5
400.	0	38	143	145	226	191	267	254	150	194	273	420	499	329	127	45	34	41	25	15	6	3	2
500.	0	19	79	55	132	124	185	185	105	130	196	312	383	279	131	47	26	26	14	8	3	1	1
700.	0	6	18	17	28	56	110	68	49	57	95	159	211	183	123	68	41	30	18	8	3	1	1
850.	0	20	50	117	140	91	83	43	46	39	61	98	128	125	111	97	84	69	46	26	11	5	5
900.	0	35	80	181	234	68	75	41	48	37	52	84	109	113	112	113	109	93	64	39	18	9	8
950.	0	54	148	266	366	111	73	46	55	39	47	74	97	111	124	145	156	140	94	59	29	17	15
1000.	0	78	222	368	582	176	73	51	62	42	44	66	90	113	144	188	217	200	133	87	45	27	24
MEAN	0	113	260	392	507	319	331	288	213	186	205	272	313	231	142	109	110	105	76	56	34	21	17

VARIANCE OF STATIONARY GEOPOTENTIAL HEIGHT(Z) FOR THE MONTH

NORTHERN HEMISPHERE 10(GPM**2)

J A N U A R Y

P(MB)	2N	6N	10N	14N	18N	22N	26N	30N	34N	38N	42N	46N	50N	54N	58N	62N	66N	70N	74N	78N	82N	86N	90N
50.	58	63	61	48	57	79	96	148	435	1049	1953	2870	3289	3530	3434	3081	2527	1940	1479	984	548	88	0
100.	67	69	73	93	113	182	209	265	590	1180	2046	2630	2695	2720	2421	2071	1827	1567	1006	802	485	189	0
200.	14	20	42	83	163	231	256	213	274	551	919	1116	1292	1416	1377	1250	1221	1073	910	805	614	198	0
300.	5	8	19	46	97	145	188	214	295	439	621	769	822	1068	1099	1063	1055	897	841	801	559	162	0
400.	2	3	8	25	51	85	128	177	292	352	471	591	697	812	823	755	779	651	639	628	421	133	0
500.	1	2	3	12	24	48	88	130	187	266	357	438	501	567	556	510	512	419	421	385	273	105	0
700.	1	0	1	3	9	22	42	65	96	143	191	215	228	230	207	145	194	140	127	52	67	45	0
850.	5	6	9	14	20	32	59	70	75	66	104	116	121	119	109	66	89	70	56	20	44	11	0
900.	9	11	19	24	29	43	86	95	91	52	75	86	95	106	108	88	100	80	53	31	58	5	0
950.	16	19	36	42	43	63	133	139	123	47	54	65	81	107	141	138	126	133	106	56	60	3	0
1000.	26	31	56	68	64	90	196	197	168	52	45	64	98	154	224	237	201	242	221	109	71	3	0
MEAN	16	22	31	40	65	94	135	165	236	381	621	816	911	986	955	859	785	655	532	425	290	85	0

* Table 1c. Variance of geopotential height resulting from stationary eddies [$\overline{Z}^{*2}$] for the month.

(units in 10^2gpm^2)

[$\overline{Z}^{*2}$]	January																(10^2gpm^2)
P(mb)	10S	5S	EQ	5N	10N	15N	20N	25N	30N	35N	40N	45N	50N	55N	60N	65N	70N	75N
50	6.4	6.4	13.6	18.7	22.2	25.8	25.6	29.2	32.3	41.0	54.1	85.9	111.4	150.4	178.3	189.8	145.0	71.8
100	1.9	3.3	6.0	7.3	9.0	11.7	13.5	14.6	21.1	41.6	75.8	136.2	191.0	223.7	257.4	253.1	209.8	124.7
200	1.6	1.6	2.9	4.3	7.0	11.7	16.9	20.0	31.4	71.7	135.8	219.3	258.4	243.6	206.5	164.1	122.1	72.5
300	.2	.7	1.4	2.3	4.0	6.3	9.1	14.3	36.6	92.7	168.2	249.5	268.9	223.8	167.7	122.5	92.5	59.4
400	.2	.3	.7	1.1	1.8	3.1	5.6	12.0	32.9	79.9	140.2	198.4	199.6	158.9	121.4	97.6	79.6	58.3
500	.2	.2	.4	.7	1.0	1.8	4.1	9.8	25.3	57.3	94.4	132.2	135.5	108.3	81.5	66.9	56.8	41.6
700	.3	.3	.3	.4	.5	.9	2.1	4.9	11.6	25.1	43.4	63.6	72.5	58.9	37.5	25.7	22.2	16.4
850	.5	.4	.3	.3	.4	.8	1.6	2.9	6.2	12.0	20.9	34.5	46.0	38.5	18.8	10.7	12.0	11.5
900	.6	.5	.4	.4	.5	.8	1.6	2.9	5.8	10.3	16.4	27.5	40.3	35.3	17.1	9.8	11.9	12.1
950	.2	.3	.4	.5	.6	.9	1.9	3.3	6.1	9.7	15.1	24.1	35.0	32.6	17.5	11.3	13.6	12.7
1000	.7	.6	.6	.6	.8	1.4	2.5	3.8	7.3	10.7	15.7	23.2	31.2	30.6	20.1	15.6	17.3	13.8
Mean	.5	.7	1.2	1.6	2.4	3.8	5.8	9.3	20.3	45.9	81.3	122.1	137.9	122.0	98.2	79.5	64.5	42.7

* As taken from Table B11b of Oort and Rasmusson (1971).

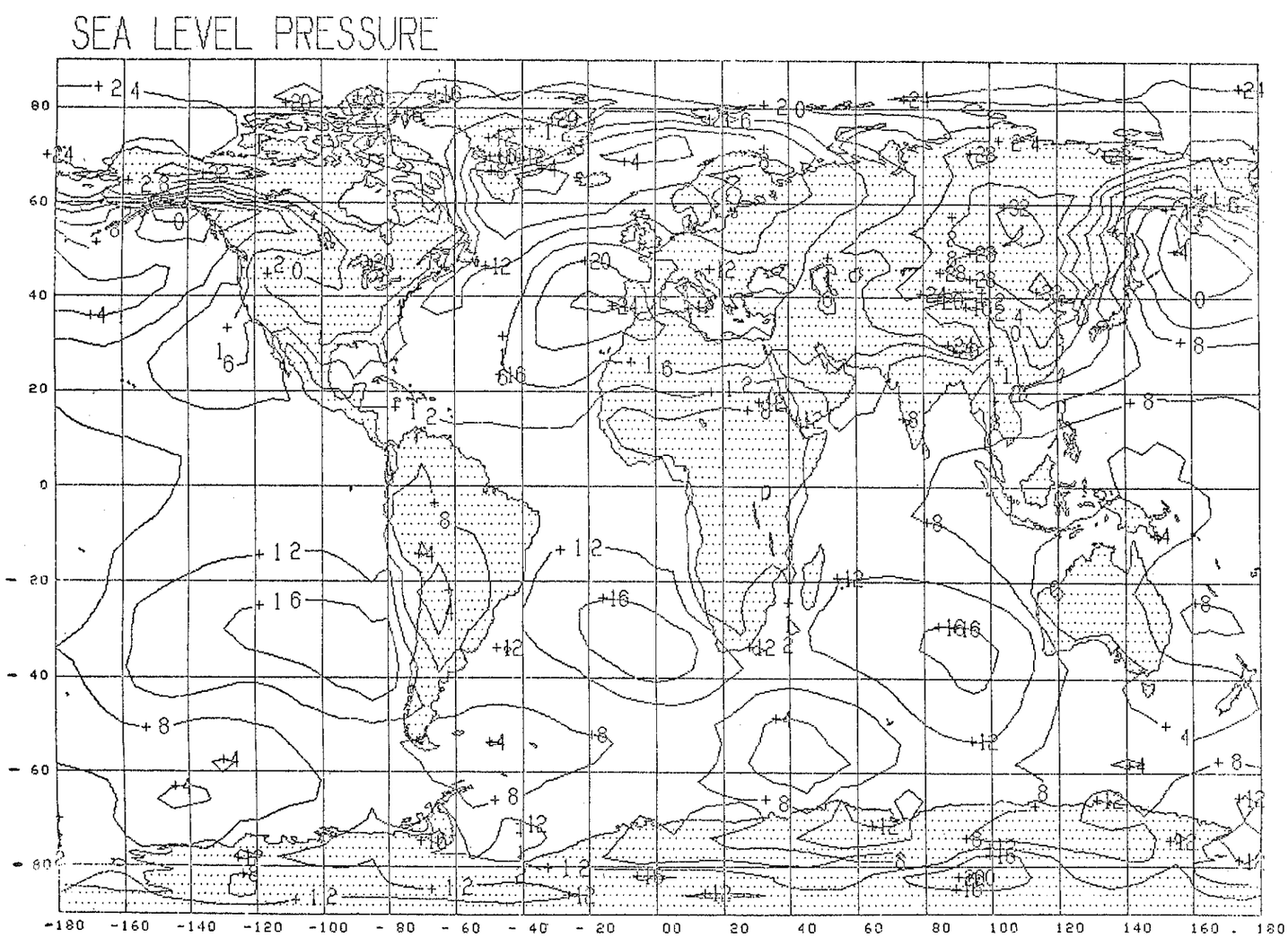

Fig. 1a. Sea level pressure plots for mean monthly January simulation with the modified GLAS model.

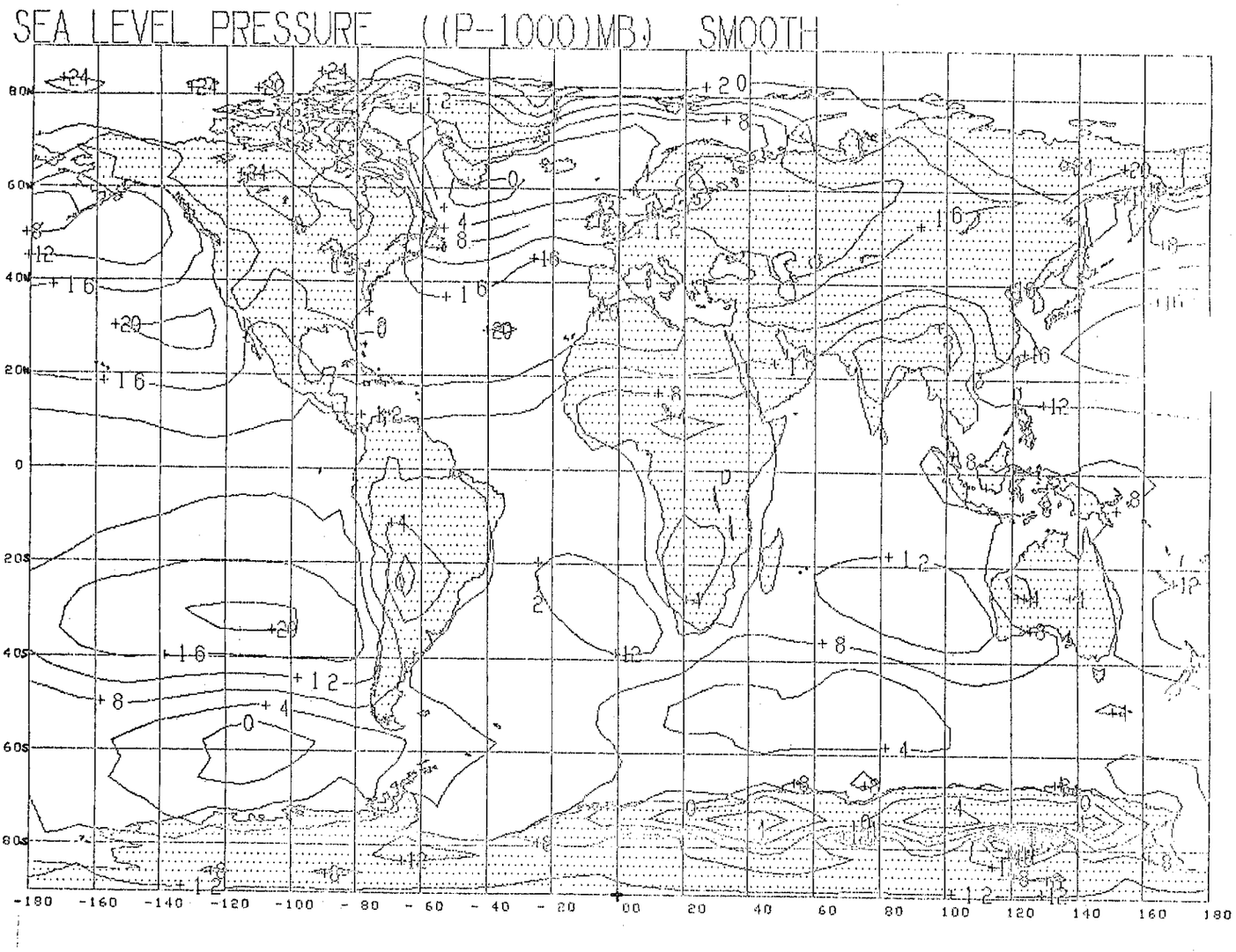

Fig. 1b. Sea level pressure plots for mean monthly January simulation with the earlier GLAS model.

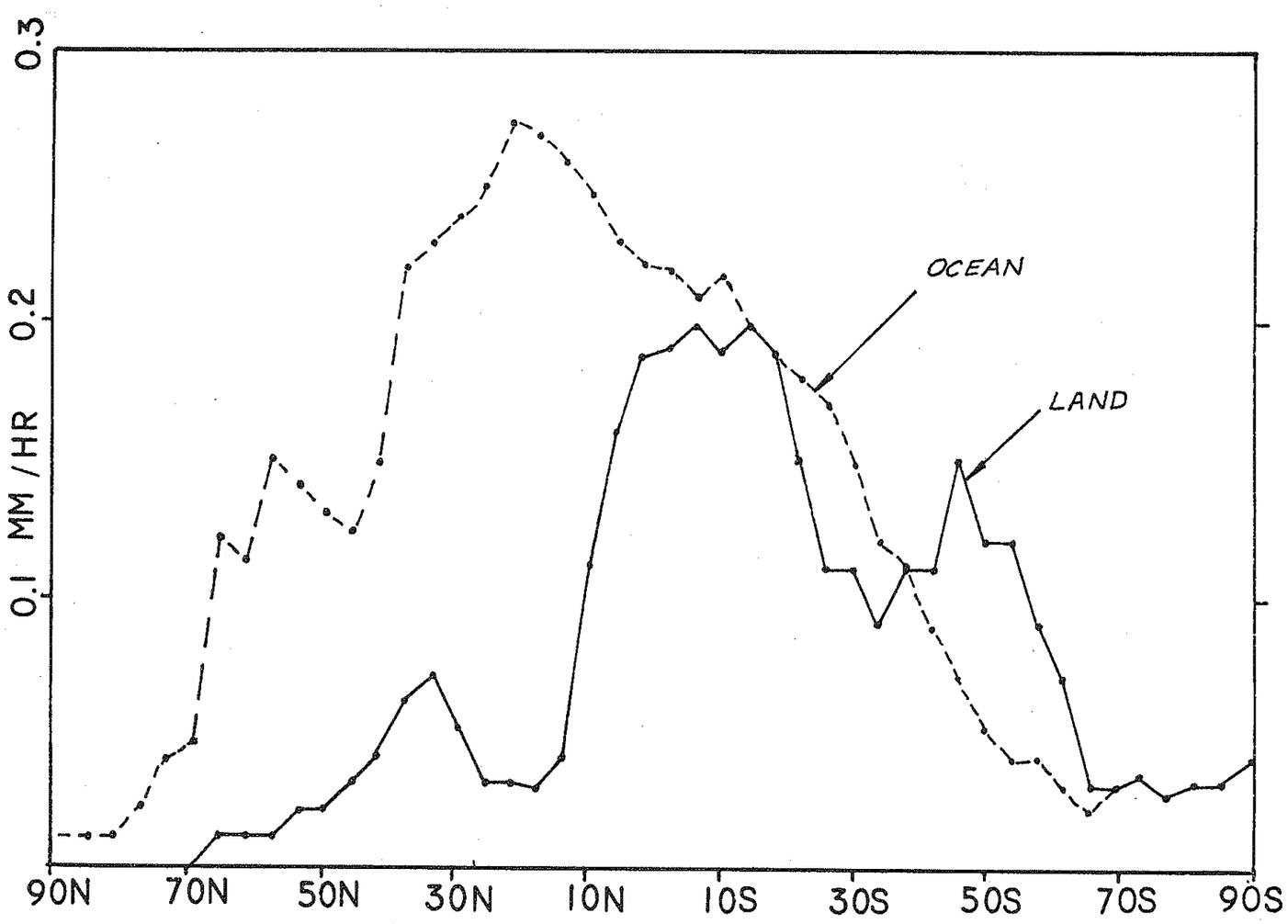

Fig. 2a. Zonal fields of evaporation over land and ocean for the modified GLAS model.

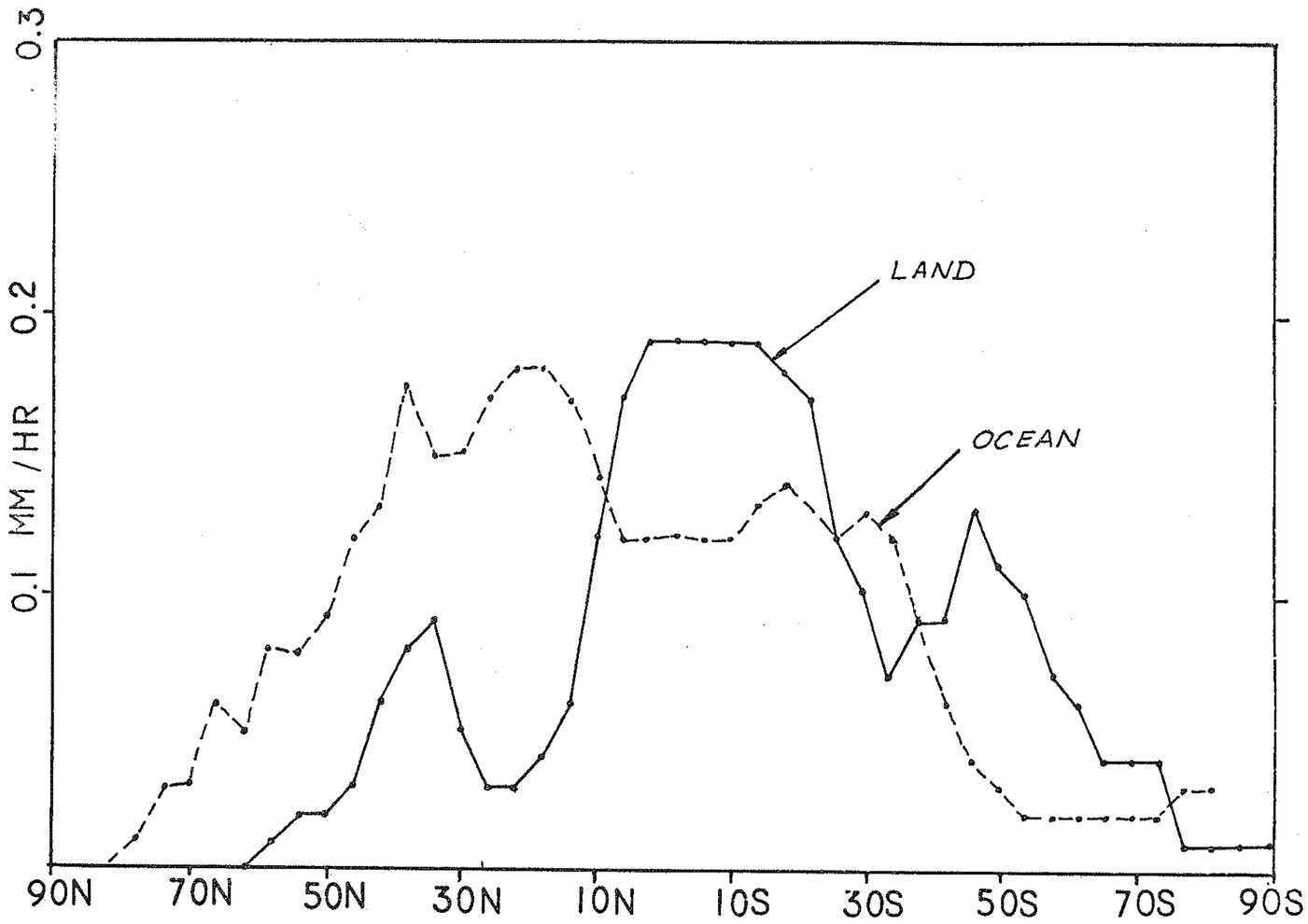

Fig. 2b. Zonal fields of evaporation over land and ocean for the earlier GLAS model.

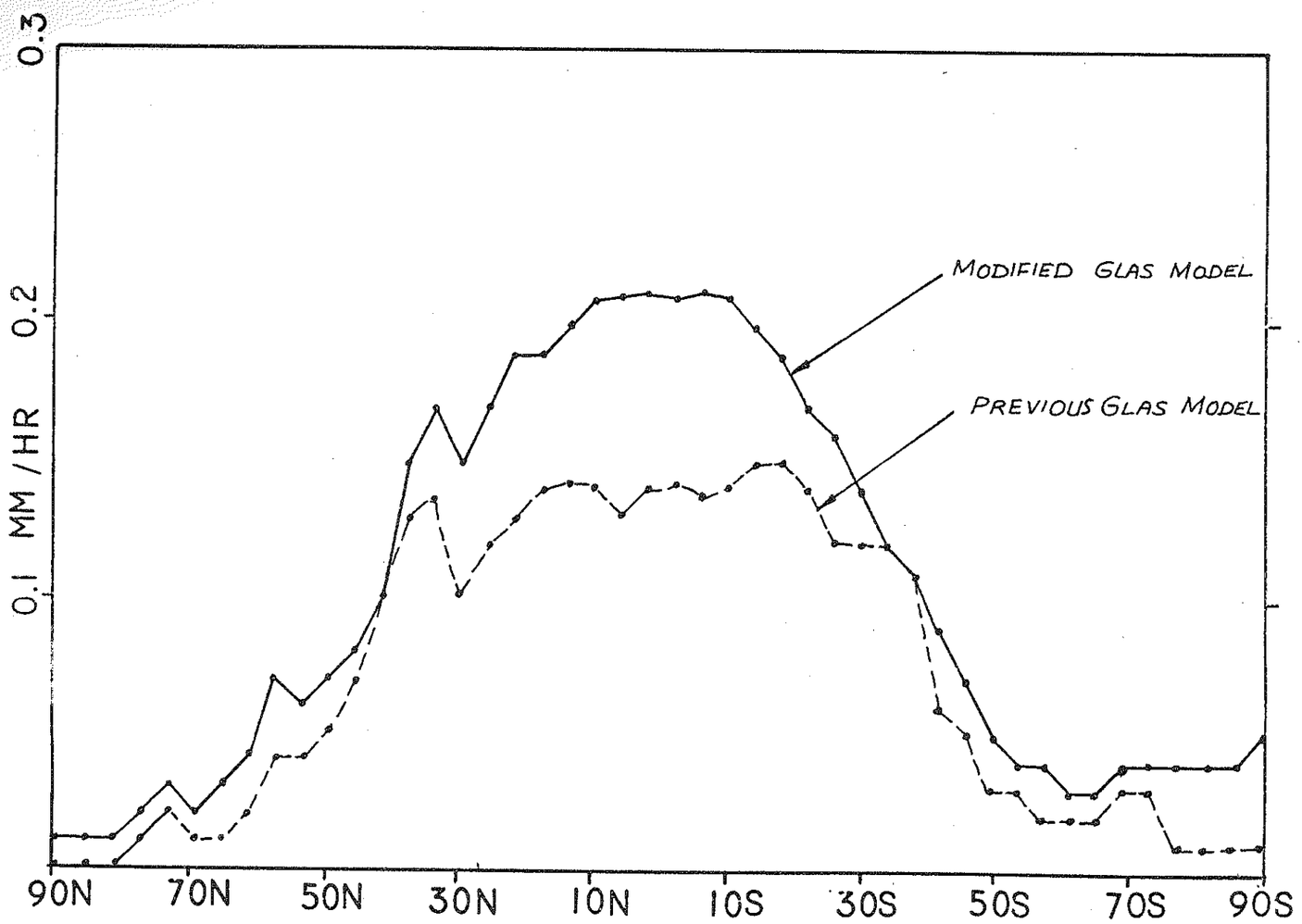

Fig. 3. Zonally averaged evaporation for the modified and earlier GLAS models.

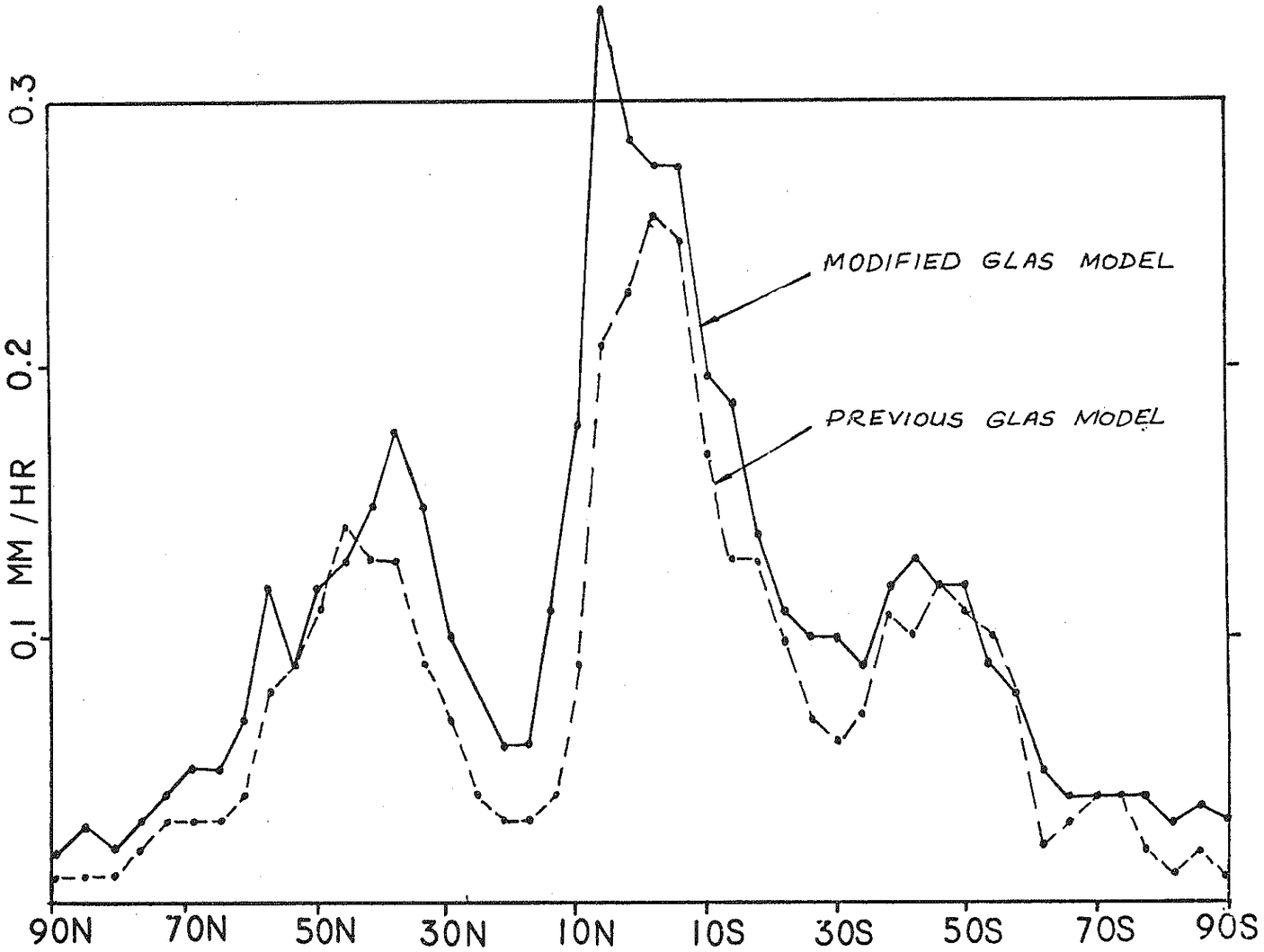

Fig. 4. Zonally averaged precipitation for the modified and earlier GLAS models.

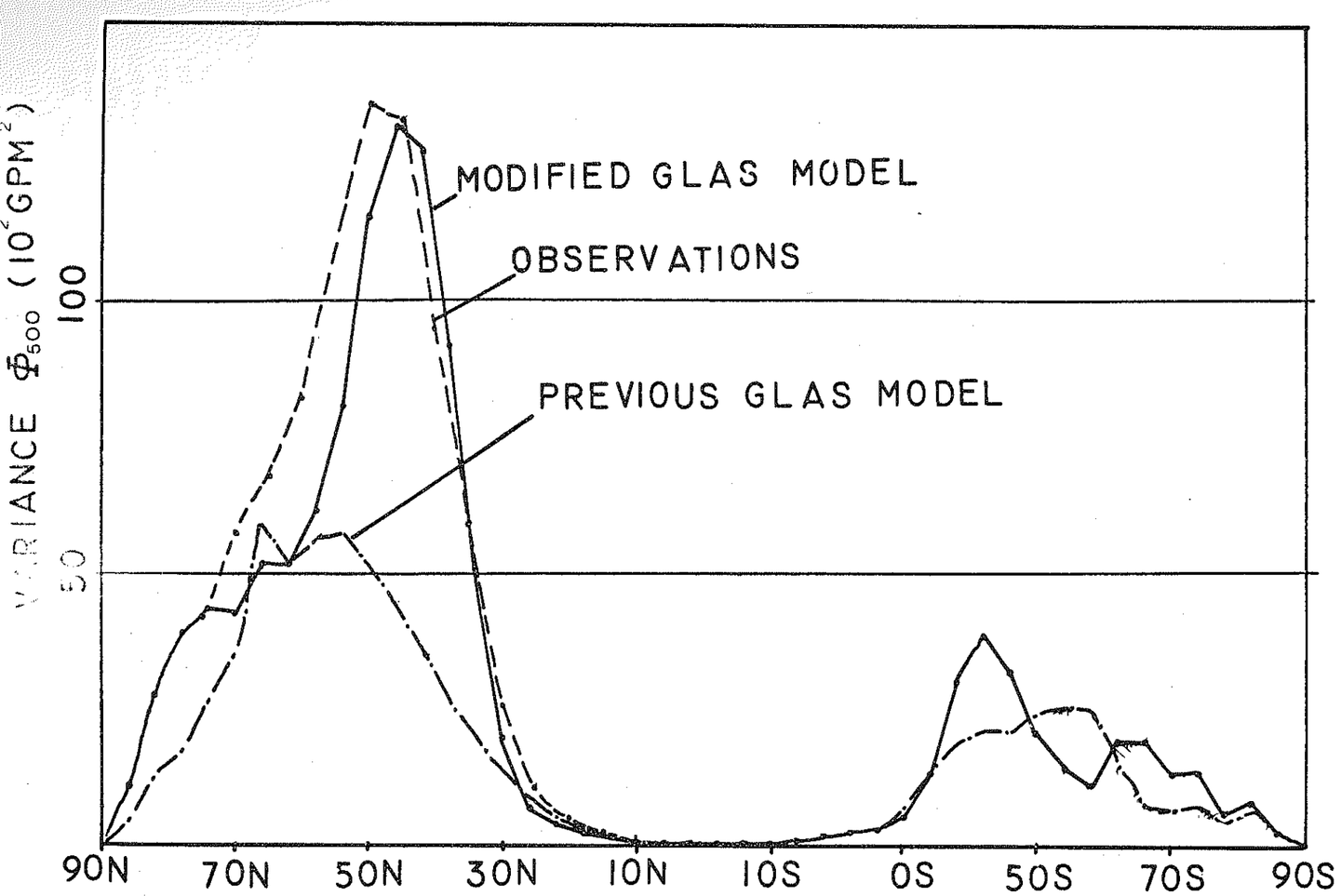

Fig. 5. Variance of 500 mb geopotential height for the modified and earlier GLAS models and observations.